WATER RESOURCES RESEARCH, VOL. 27, NO. 1, PAGES 77–90, JANUARY 1991

Light Stable Isotope Systematics of Large-Scale Hydrologic Regimes in California and Nevada

NEIL L. INGRAHAM[1] AND BRUCE E. TAYLOR[2]

Department of Geology, University of California, Davis

Surface waters, shallow groundwaters, and precipitation samples were collected along three traverses, which begin at the California coast and are oriented in an east-west manner, roughly parallel to the atmospheric flow path of meteoric water. The hydrogen isotope compositions from short-term precipitation records varied as much as 40‰ at one location and were not representative of the average annual isotopic composition of precipitation. The hydrogen isotope ratios of surface waters and shallow groundwaters distinguish segments with isotopic variations that correlate with measured vertical fluxes of meteoric water. One coastal segment appears to closely approximate an open system in which precipitation dominates over evapotranspiration. Most segments are described by rather regular variations in δD: 3–45‰ per 100 km, which represent different degrees of closure of the hydrologic system caused by variable partitioning of precipitation between runoff and evapotranspiration. All partially closed systems imply terrestrial recycling of water. A simple model estimates this amount to be about 20% across northern and central California. Three segments, representing the Great Basin, show virtually no geographic variation and appear to represent isotopically closed systems.

INTRODUCTION

West-to-east variations in the oxygen and hydrogen isotope composition of surface waters and shallow ground waters across northern California and Nevada reflect general isotopic changes in atmospheric water vapor accompanying continued precipitation and recycling of water by evapotranspiration upwind [*Ingraham and Taylor*, 1986]. These variations, modeled in terms of isotopic fractionation in open and closed hydrologic systems, indicated a discrepancy in the measured and Rayleigh model-predicted hydrogen isotope compositions of inland meteoric water which was attributed to recycling. The results of the present study incorporate measurements across central and southern California, and reveal additional complexities.

Reconnaissance hydrogen isotope studies by *Friedman et al.* [1964] indicate the profound effects of geography (primarily distance inland and elevation) on the compositions of surface waters in the United States. *Friedman and Smith* [1970, 1972] studied the hydrogen isotope composition of precipitation and reported an orographic effect across the Sierra Nevada of 40‰ per 1000 m in elevation. Later, *Smith et al.* [1979] found highly variable deuterium contents in precipitation in central California, with differences in δD ranging from up to 114‰ between sequential samples from the same storm collected at one station to up to 37‰ for the mean values of δD of individual storms at 13 stations. They modeled the change in isotopic composition of average precipitation in southeastern California and western Nevada from a pseudoadiabatically cooling air mass. Their model did not include prior precipitation over the ocean or upwind evapotranspirational return and recycling of water.

In a study of water balance in the Amazon Basin, *Salati et al.* [1979] determined the oxygen isotope composition of precipitation in the basin and found a very small (0.075‰ per 100 km) isotopic depletion with distance inland from the Atlantic Ocean. They attributed the small depletion to a large contribution from reevaporated moisture. Similarly, *Rozanski et al.* [1982*a*] modeled the stable isotope composition of atmospheric water vapor and precipitation in central Europe with respect to distance from the Atlantic Ocean and included the effects of winter precipitation and summer evapotranspiration. They documented decreases in δD of 3.3‰ per 100 km in winter precipitation and 1.3‰ per 100 km in summer precipitation. *Rozanski et al.* [1982*b*] concluded that variations in local precipitation were primarily controlled by regional-scale precipitation/evapotranspiration events upwind, modified only slightly by local temperature fluctuations. Based on this, *Rozanski* [1985] interpreted the isotopic composition of old European groundwaters as indicating atmospheric circulation patterns similar to those of the present. *Yonge et al.* [1989] studied the stable isotopic ratios of surface waters across western Canada to the Great Divide and beyond. These researchers modeled the results from over 500 km distance inland in terms of a single-stage Rayleigh distillation curve and concluded that precipitation west of the divide did not appear to be greatly affected by evapotranspiration.

The present study bears on the history of meteoric water in hydrologic regimes dominated by an eastward atmospheric flux across California and Nevada. Variations in stable isotope ratios of surface waters and shallow groundwaters on a regional scale can be modeled effectively in terms of precipitation, evapotranspiration, and runoff. This approach includes a somewhat larger view of the hydrologic cycle than most previous models, which have emphasized the precipitation-dominated orographic effects.

[1]Now at Water Resources Center, Desert Research Institute, University of Nevada, Las Vegas.
[2]Now at Geological Survey of Canada, Ottawa, Ontario.

Paper number 90WR01708.
0043-1397/91/90WR-01708$05.00

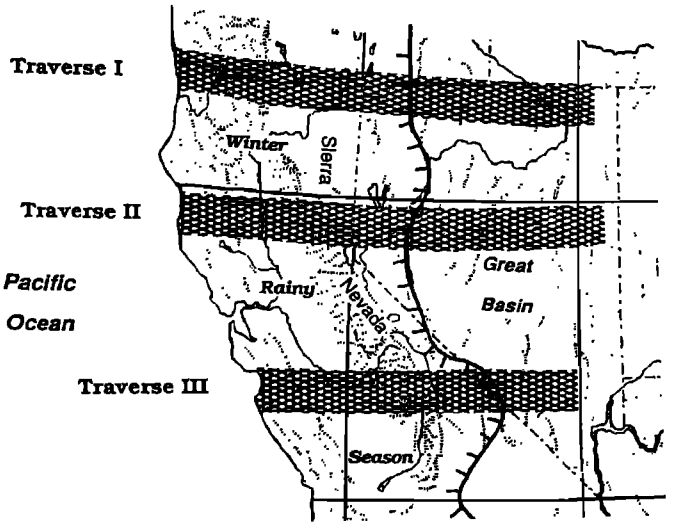

Fig. 1. Location of the three east-west traverses used in this study. The traverses were positioned parallel to the atmospheric flow path and located to include most major physiographic and hydrologic provinces in California and Nevada. Also shown is the region of dominantly winter precipitation [after *Markham*, 1970].

METHODS

Sample Collection

All samples were collected in 125 ml (4 oz.) polysealed glass bottles along three east-west traverses across California and Nevada (Figure 1). The traverses were aligned in a manner to determine the maximum changes in isotopic composition in meteoric water as it migrates from west to east. The traverses were approximately equispaced and included most major physiographic and hydrologic provinces in California and Nevada, including the Great Basin. Shallow groundwaters were considered to be the type of sample that best represented average precipitation, being the least sensitive to the extreme yearly, seasonal, and in-storm isotopic variability (such as found by *Smith et al.* [1979]) and yet reflecting the current climate and hydrologic regime.

Groundwaters

Eighty-five samples of shallow groundwater (including some surface waters) were collected for this study. An additional 35 isotopic analyses of groundwater reported in the literature were incorporated in the data base.

Precipitation

Precipitation (as rain and snow) was collected to compare with the surface water and shallow groundwater samples and to determine the stable isotope composition of waters available for infiltration. Rain was collected along the coastal portion of traverse I and also along traverse II in California from 0 to 250 km inland. Rain samples were collected by a simple device consisting of a 2 L plastic bottle set inside a nursery can backfilled with soil for stability. Tygon tubing with a restriction was attached to a funnel and placed through a stopper in the neck of the bottle. A short length (15 cm) of tygon tubing (0.8 mm ID) was inserted through a hole in the stopper to release air displaced by water as the bottle filled. The small-diameter tubing restricted evaporation of the sample.

Thirty-nine such rain samplers were placed in selected locations along the two traverses (I and II). Four sets of samples were collected along traverse II and one along traverse I. The rainwater caught in the collectors was measured volumetrically, and an aliquot was stored for analysis. Several duplicate samplers were left undisturbed the entire season (November to April) to collect the complete record of rain, which compared well both volumetrically and isotopically to the summation of the short-term data.

Six early spring snow cores were collected along portions of traverse II in the Sierra Nevada of California, where precipitation occurs primarily as snow. The snow was cored using a modified Mt. Rose snow sampler and sealed in plastic containers and allowed to melt slowly. The meltwater was then bottled, in the same manner as with other water samples.

Isotopic Analysis

Both the hydrogen and oxygen isotope ratios were determined using two different methods. Quantitative conversion of water to hydrogen gas was performed using both uranium [*Bigeleisen et al.*, 1952] and zinc [*Kendall and Coplen*, 1985]. In the uranium method, hydrogen was Toepler-pumped into a Pyrex glass tube (3/8 in OD × 12 in), sealed with a torch, and stored for several weeks for analysis. With zinc, hydrogen gas was produced and sealed in the same Pyrex tube (1/4 in OD × 6 in) used for reaction. The oxygen isotope analysis of water was accomplished principally by the CO_2 equilibration method [*Epstein and Mayeda*, 1953] but also by the guanidine hydrochloride method [*Dugan et al.*, 1985]. An equilibrium oxygen isotope CO_2–H_2O fractionation factor of 1.0412 (at 25°C) was used for the CO_2 equilibration technique [*Freidman and O'Neil*, 1977]. All data are reported in the standard δ notation with respect to SMOW. The reproducibility of δD is about 1‰ and of $\delta^{18}O$ is about 0.2‰.

RESULTS

Groundwaters

The stable isotope compositions of all surface waters and shallow groundwaters collected for this study are listed in Table 1 and plotted by traverse in Figure 2. For the most part the data plot close to, but consistently below, the present-day meteoric water line (MWL) ($\delta D = 8\delta^{18}O + 10$; *Craig* [1961]). However, some samples were collected from thermal springs and do not plot on the MWL, having undergone varying degrees of oxygen isotope exchange with the host rock at depths. The δD values of the spring samples still carry the signature of meteoric water, since boiling is not observed, and evaporative steam loss does not affect the isotopic data [cf. *Truesdell et al.*, 1977].

Some of the data taken from the literature are for waters from the Great Basin with apparent ^{14}C ages ranging from 11,000 to 28,200 years, and hence, the infiltration of these waters may have occurred under slightly different climatic conditions. Hydrogen isotope compositions of paleowater samples depleted by more than about 5‰ relative to present-day meteoric water are thought to reflect a colder and more humid climate [*Merlivat and Jouzel*, 1979]. Nevertheless, these older waters do not deviate significantly from modern samples with respect to the regional variations discussed.

TABLE 1. Stable Isotope Compositions of All Surface Waters and Shallow Groundwaters

Distance From Coast, km	Occurrence	Collection Date	Location	δD_{SMOW}	$\delta^{18}O_{SMOW}$
		Traverse I			
0.2	Roadcut Spring	July 1983	T10N/R1E/31	−52	−7.4
3	stream	July 1983	T12N/R1E/23	−50	−7.6
15	Roadcut Spring	July 1983	T17N/R2E/26	−56	−7.7
30	Roadcut Spring	July 1983	T17N/R3E/9	−63	−8.6
36	Roadcut Spring	July 1983	T6N/R4E/15	−71	−9.8
38	Roadcut Spring	July 1983	T18N/R4E/4	−69	−9.1
73	Waters Creek, Oregon	July 1983	T37S/R7W/9	−78	−10.2
97	irrigation well	July 1983	T42N/R49W/17	−94	−11.5
102	Canyon Creek, Oregon	July 1983	T30S/R5W/35	−79	−10.1
127	irrigation well, Oregon	July 1983	T34S/R1W/4	−96	−12.4
134	Drew Creek, Oregon	July 1983	T31S/R1W/32	−87	−11.4
137	Stewart Spring	July 1983	T41N/R6W/2	−101	−12.2
151	Big Spring	July 1983	T40N/R4W/9	−108	−14.4
156	Tubbs Spring, Oregon	July 1983	T39S/R5E/32	−104	−13.4
185, R	Hunt Hot Spring	Aug. 1973	T37N/R1W/25	−94	−13.3
207	irrigation well, Oregon	July 1983	T39S/R8E/23	−96	−10.8
256	irrigation well, Oregon	July 1983	T36S/R12E/22	−123	−15.3
256H	Bieber Hot Spring	July 1983	T38N/R7E/12	−119	−14.5
269H	Canby Hot Spring	July 1983	T42N/R10E/28	−117	−13.6
282	Rush Spring	Aug. 1985	T40N/R10E/24	−103	−14.0
315	Stow Spring	July 1983	T43N/R15E/27	−102	−14.6
320	Mineral Spring	Aug. 1983	T47N/R15E/1	−111	−15.2
322, R	Leonards Hot Spring	July 1973	T43N/R16E/13	−117	−13.8
328H	Menlo Hot Spring	Aug. 1983	T39N/R17E/20	−117	−14.8
328H	Lakeview Hot Spring, Oregon	Aug. 1983	T39S/R20E/9	−125	−13.6
350	Windmill, Vya	Aug. 1983	T42N/R19E/4	−119	−14.6
385	High Rock Cnyn Spring	Aug. 1983	T40N/R23E/16	−115	−14.7
400H	Hot Spring, Soldier Meadows	Aug. 1983	T40N/R24E/22	−129	−16.5
400H	Hot Spring, Soldier Meadows	Aug. 1983	T40N/R24E/22	−129	−16.5
405H, M	Gerlach Hot Spring	...	T42N/R23E/2	−121	−14.7
412H, M	Hot Spring, Soldier Meadows	...	T40N/R24E/23	−130	−16.6
435H, M	Bog Hot Spring	...	T46N/R28E/18	−124	−15.3
440H, M	Harney Lake Hot Spring	...	T27S/R29E/36	−129	
450H, M	flowing well	...	T46N/R28E/13	−126	−15.6
450H, M	Baltazor Hot Spring	...	T46N/R28E/13	−125	−15.3
460H, M	Dyke Hot Spring	...	T43N/R30E/25	−128	−16.3
465H, M	Trout Creek Hot Spring	...	T39S/R37E/16	−127	−16.2
480H, M	Howard Hot Spring	...	T44N/R31E/4	−127	−16.2
530H, M	McDermit Hot Spring	...	T41N/R41E/20	−135	−16.5
565H	Golconda Hot Spring	July 1983	T36N/R40E/29	−131	
665	Beowawe Hot Spring	July 1983	T31N/R48E/8	−130	−14.8
700	Carlin Hot Spring	July 1983	T33N/R52E/33	−133	
800H, M	White Pine Hot Spring	...	T23N/R63E/6	−128	−16.2
		Traverse II			
0.4	Roadcut Spring	May 1984	T18N/R17W/18	−37	−5.4
0.7	Roadcut Spring	May 1984	T18N/R17W/18	−40	−5.6
9	Horse Trough Spring	May 1984	T16N/R16W/9	−42	−6.2
15.5	Comptche Spring	May 1984	T16N/R16W/12	−44	−5.9
30	creek	May 1984	T18N/R15W/15	−48	−6.7
31	Montgomery Woods Spring	May 1984	T16N/R14E/15	−45	−6.6
63	Blue Lake Spring	May 1984	T15N/R10W/6	−58	−7.9
90	Bartlett Spring	May 1984	T15N/R8W/2	−68	−8.4
107	Barrel Spring	May 1984	T15N/R5W/25	−66	−8.5
107	Barrel Spring	May 1984	T15N/R5W/25	−65	−8.6
110	domestic well	May 1984	T15N/R5W/4	−58	−8.4
150	domestic well	May 1984	T16N/R2W/33	−64	−8.4
200	domestic well	May 1984	T16N/R5E/16	−59	−8.4
200	domestic well	May 1984	T16N/R5E/16	−59	−8.5
221	domestic well	May 1984	T16N/R7E/13	−69	−9.9
225	Bitney Spring	May 1984	T16N/R8E/20	−68	−9.8
232	spring	May 1984	T17N/R8E/25	−71	−9.6
249	White Cloud Spring	May 1984	T17N/R10E/22	−77	−10.5
254	Skillman Spring	May 1984	T17N/R11E/30	−74	−10.4
261	Roadcut Spring	May 1984	T17N/R11E/22	−78	−10.7
261	spring	May 1984	T20N/R11E/25	−89	−11.8
282	spring	May 1984	T20N/R14E/31	−105	−13.7

TABLE 1. (continued)

Distance From Coast, km	Occurrence	Collection Date	Location	δD_{SMOW}	$\delta^{18}O_{SMOW}$	^{14}C Age
		Traverse II (continued)				
285	Roadcut Spring	May 1984	T19N/R14E/24	−94	−12.5	
294	Donner Summit Spring	May 1984	T17N/R15E/8	−91	−13.5	
298	Hennes Pass Spring	May 1984	T19N/R15E/14	−103	−13.5	
323	Farad Warm Spring	July 1984	T19N/R18E/30	−111	−13.8	
325H	Tressel Hot Spring	July 1984	T21N/R17E/11	−115	−15.1	
336H, M	Steamboat Hot Spring	...	T18N/R20E/33	−117	−12.2	
390H, M	Fernly Hot Spring	...	T20N/R26E/18	−122	−13.3	
410H, M	Lee Hot Spring	...	unsurveyed	−126	−13.2	
470	Kyle Spring	Oct. 1985	...	−123		
480H, M	Dixie Hot Spring	...	T22N/R35E/8	−126	−15.9	
485,J	Flowing Well, Dixie Valley	May 1979	T21N/R35E/10	−130	−16.3	
530H, M	Smith Creek Hot Spring	...	T17N/R39E/11	−130	−16.7	
585H, M	Spencer Hot Spring	...	unsurveyed	−136	−16.0	
640H, M	Bartholomae Hot Spring	...	T18N/R50E/28	−128	−16.3	
750H, M	Monte Neva Hot Spring	...	T21N/R63E/24	−128	−16.7	
755H, M	Cherry Creek Hot Spring	...	T23N/R63E/6	−128	−16.2	
		Traverse III				
20	irrigation well	June 1984	T14S/R3E/25	−43	−5.7	
22	irrigation well	June 1984	T14S/R4E/19	−40	−4.9	
26	irrigation well	June 1984	T15S/R4E/9	−46	−6.2	
50	irrigation well	June 1984	T14S/R6E/14	−43	−5.6	
54	irrigation well	June 1984	T14S/R6E/25	−47	−6.3	
60	artesian well	June 1984	T18S/R7E/17	−53	−6.6	
74	irrigation well	June 1984	T15S/R9E/17	−61	−8.0	
84H	Mercy Hot Spring	June 1984	T14S/R10E/15	−57	−5.4	
87	irrigation well	June 1984	T15S/R10E/23	−64	−7.8	
97	irrigation well	June 1984	T13S/R11E/26	−71	−9.8	
122	irrigation well	June 1984	T14S/R14E/1	−73	−9.8	
172	irrigation well	June 1984	T14S/R17E/2	−79	−10.1	
261	spring	June 1984	T14S/R27E/11	−96	−12.8	
268	Redwood Creek	June 1984	T14S/R28E/9	−88	−11.4	
292	Kings River	June 1984	T13S/R30E/17	−107	−14.0	
308	Matlock Lake	June 1984	T13S/R33E	−101	−13.4	
311	Onion Creek	July 1984	T13S/R34E	−109	−14.7	
320	irrigation well	July 1984	T10S/R34E/16	−101	−13.4	
327	spring	July 1984	T8S/R35E/17	−123	−15.9	
350	irrigation well	July 1984	T5S/R37E	−126	−16.1	
400	Scottys Castle Spring	July 1984	T11S/R42E/1	−112	−14.1	
420	Stovepipe Wells	July 1984	T15S/R45E/16	−107	−13.3	
420	Stovepipe Wells	July 1984	T15S/R45E/16	−105	−13.1	
445W	Travertine Spring	...	T29N/R1E/23	−109		
445W	Texas Spring	...	T29N/R1E/15	−108		23,100
445W	Nevares Spring	...	T28N/R2E	−109		24,000
457H	Beatty Hot Spring	July 1984	T12S/R47E/8	−112	−14.3	
457	domestic well	July 1984	T12S/R47E/8	−112	−14.2	
472W	well	...	...	−108	−14.2	17,000
490W	well	...	...	−104	−13.0	11,000
515W	well	...	...	−114		28,200
515W	well	...	...	−107	−13.0	22,900
520W	well	...	...	−114		14,800
575W	Hiko Spring	...	...	−113		22,000
580W	Crystal Spring	...	...	−109	−14.3	20,500

W, *Waddell et al.* [1984]; M, *Mariner et al.* [1975]; J, *Jacobson et al.* [1983]; R, *Reed* [1975]. H, samples collected from hot springs (T > 40°C). Where available, ^{14}C ages are listed.

The δD values of samples from each traverse are plotted, in Figure 3, versus latitudinal distance from the Pacific Ocean. The traverses are divided into segments to indicate hydrologic regimes of differing isotopic characteristics. The northernmost traverse (traverse I) contains three distinct segments, or regimes, while the other two traverses each contain four. The isotopic variations of surface waters and shallow groundwaters between segments may be compared to variations in precipitation [*Goodridge et al.*, 1981], potential evapotranspiration, as measured from Class A evaporation pans [*MacGillivray et al.*, 1975], and elevation. There may be fine structure to the isotopic "trends," and the regression lines greatly simplify the observed variations. However, the trends described are useful for comparison and form a basis for discussion of large-scale processes.

Segment I-a displays a marked, curvilinear decrease in

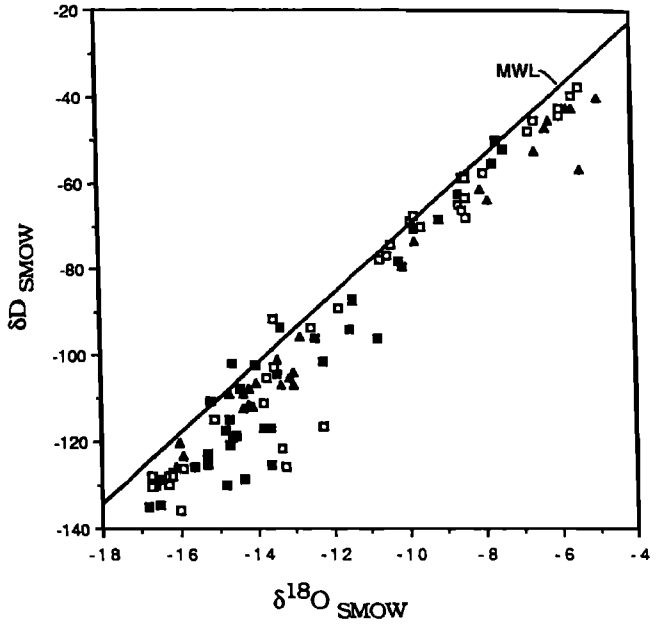

Fig. 2. Plot of δD versus $\delta^{18}O$ of surface waters and shallow groundwaters on traverse I (solid squares), traverse II (open squares), and traverse III (solid triangles), collected for this study. The meteoric water line $\delta D = 8\delta^{18}O + 10$ is also shown.

δD, from −50 to almost −85, for an average depletion of 60‰ per 100 km. Segments representing the Great Basin (I-c, II-d, and III-d), a vast area of interior drainage, show little further decrease in δD with distance from the coast. All other segments appear to be more regular, linear depletion trends of various slopes.

The isotopic variation within each segment appears continuous on a large scale, and each segment adjoins another, except for segment "d" of traverse III. The average δD of water samples from segment III-d (approximately −110‰) marks an abrupt increase of about 20‰ from the terminus of segment III-c (−125 to −130‰).

Precipitation

All precipitation samples were analyzed for their hydrogen isotopic compositions, and most were analyzed for their oxygen isotopic compositions. Table 2 lists the type of precipitation collected (rain or snow), date of collection, distance from the coast, amount collected (in centimeters), and isotopic compositions.

Traverse I. The amount of rain recorded at the Crescent City weather station during the period of collection (January 20 to March 30, 1985) varied from 73% (February) to 85% (March) of normal. The hydrogen isotope data for rain samples are shown with respect to distance from the Pacific Ocean measured along a line of latitude, in Figure 4. The data exhibit as much as a 40‰ per 50 km decrease in δD with distance from the coast. The decrease is continuous and appears to exhibit a large curvilinear trend as found for surface waters and shallow groundwaters along segment I-a.

Traverse II. All pairs of the hydrogen and oxygen isotope data of rain collected along traverse II are plotted in Figures *5a–5d* for each individual sampling run versus distance inland. The rain samples were produced from the same storm system and are connected in a fashion which tracks the position of the storm as it passes across the coast, heading eastward across the state. A general pattern of decreasing δD with distance inland (comparable to that in shallow groundwaters) is apparent, but the δD of precipitation collected at one location may vary up to 40‰ between sample sets.

However, the oxygen-hydrogen isotope equilibrium relationship is frequently interrupted by excursions of the data from the MWL, typically above the line. These deviations may represent the effects of nonequilibrium, kinetically controlled isotopic fractionation of the storm's water mass, or portions thereof, by recondensation and mixing of evaporated water in isotopically inhomogenous storm cells. The stable isotopic data of short-term rain samples are generally less effective in defining hydrologic regimes than are data on surface waters and shallow groundwater.

The weighted average hydrogen isotope composition of precipitation and the hydrogen isotope compositions of the snow samples from traverse II are plotted with the hydrogen isotope compositions of surface waters and shallow groundwaters in Figure 6. The large-scale variations in the weighted average δD values of precipitation correspond closely with the δD values of the surface waters and shallow groundwaters, which suggest that surface waters and shallow groundwaters tend to average out yearly, seasonal, and in-storm as well as small geographic variations of the isotopic composition of precipitation. However, both the rain and snow appear to be slightly depleted in deuterium relative to surface waters and groundwaters at the same locations, perhaps due to slight evaporation of meltwater prior to infiltration.

DISCUSSION

Atmospheric condensation is thought to occur under equilibrium conditions [e.g., *Dansgaard*, 1964], controlled largely by Rayleigh distillation. The hydrogen isotope composition of the precipitation can be expressed by $\delta D = (F_v^{\alpha-1} - 1) \times 1000$ where F_v is the fraction of water vapor remaining in the cloud, and α is the temperature-dependent fractionation factor for deuterium between the liquid and vapor.

The results of isotopic analysis of groundwaters and weighted average precipitation along traverses across California and into Nevada reflect a common set of meteorological processes. The most important processes causing the isotopic fractionation are precipitation and evapotranspiration. Initial results of a study of eastward moving moisture in northern California and Nevada [*Ingraham and Taylor*, 1986] indicated that precipitation dominated initially but soon gave way to increasing evapotranspiration. Isotopic variations in central and southern California can be similarly modeled, but additional complications must be considered.

As discussed here, the boundaries of the system are broadened beyond those of the cloud (as the system is usually described in a precipitation-dominated model) to include the ground surface to a shallow depth beneath. Therefore shallow groundwaters are thought generally to reflect the isotopic composition of the system, as defined.

In this expanded system the eastward moving moisture becomes depleted in deuterium by continued precipitation. If all precipitation were removed from the system via runoff, leaving none to be recycled back to the atmosphere by

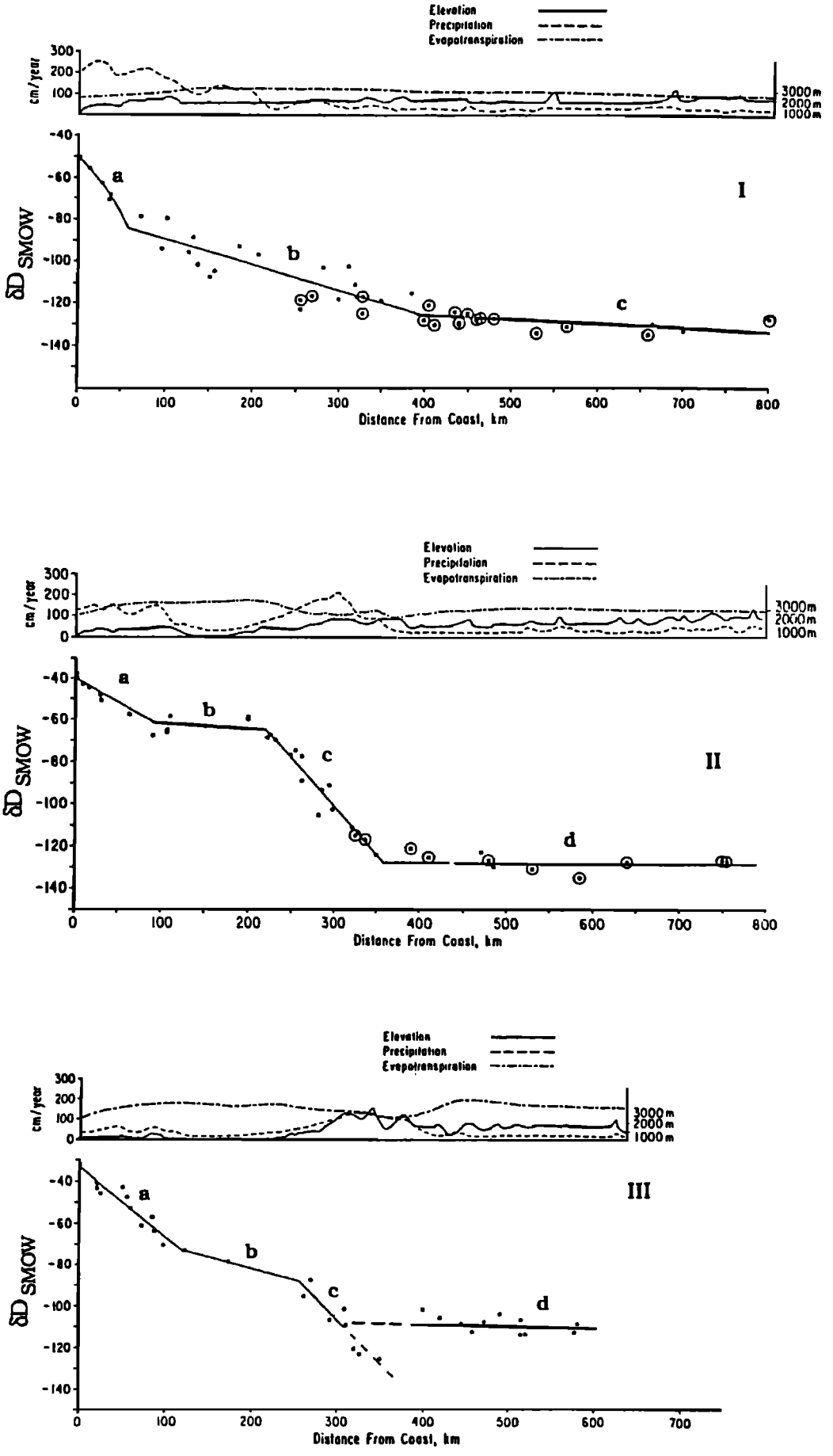

Fig. 3. Plot of δD versus distance from the Pacific Ocean of traverses I–III. Precipitation data [*Goodridge et al.*, 1981], evapotranspiration data [*MacGillivray et al.*, 1975], and topography are also shown. The segments, a, b, c, and d and their regression curves (solid curves in the figures) are discussed in the text. Circled data points represent samples from thermal (temperature > 40°C) springs.

TABLE 2. Analysis of Precipitation Samples

Distance From Coast, km	Date Collected	Location	Amount of Rain Collected or Snow Depth, cm	δD_{SMOW}	$\delta^{18}O_{SMOW}$
		Traverse I			
8	March 31, 1985	T16N/R1W/2	10.4	−54	−7.3
12.7	March 31, 1985	T16N/R1E/8	3.6	−54	−7.9
30	March 31, 1985	T17N/R3E/10	13.2	−70	−10.1
37	March 31, 1985	T18N/R4E/9	7.7	−78	−11.4
45	March 31, 1985	T33S/R5E/9, Ore	8.6	−89	−13.0
73	March 31, 1985	T37S/R7W/9, Ore	6.7	−93	−13.3
		Traverse II, Rain			
1	Nov. 11, 1984	T18N/R17W/7	21.8	−32	−53
1	Dec. 9, 1984	T18N/R17W/7	18	−60	−8.7
1	Jan. 20, 1985	T18N/R17W/7	7	−53	−7.0
1	March 31, 1985	T18N/R17W/7	1.8P	−72	−8.1
35	Nov. 12, 1984	T16N/R13W/28	15.4	−47	−7.1
35	Dec. 9, 1984	T16N/R13W/28	19.2	−76	−11.2
35	Jan. 20, 1985	T16N/R13W/28	1.9P	−69	−10.0
72	Dec. 9, 1984	T15N/R9W/17	19	−75	−11.8
72	Jan. 20, 1985	T15N/R9W/17	4.9	−82	−11.3
72	March 31, 1985	T15N/R9W/17	25.9	−73	−10.8
85	Jan. 20, 1985	T15N/R8W/9	8.7	−89	−12.7
85	March 31, 1985	T15N/R8W/9	26.8	−83	−12.7
96	Dec. 9, 1985	T15N/R6W/11	23.1	−80	−11.4
96	Jan. 20, 1985	T15N/R6W/11	6.6	−100	−12.0
96	March 31, 1985	T15N/R6W/11	26.8	−78	−11.2
107	Nov. 12, 1984	T15N/R5W/25	17.9	−53	−10.0
107	March 31, 1985	T15N/R5W/25	17.1	−78	−12.7
112	Nov. 12, 1984	T15N/R5W/3	8.1	−57	−10.2
112	Dec. 9, 1984	T15N/R5W/3	14.1	−76	−11.6
112	Jan. 19, 1985	T15N/R5W/3	3.6	−9.9	−13.4
112	March 31, 1985	T15N/R5W/3	15.6	−81	−12.0
120	Nov. 12, 1984	T15N/R4W/18	5.8	−57	−9.8
120	Dec. 9, 1984	T15N/R4W/18	8.5	−80	−11.2
120	Jan. 19, 1985	T15N/R4W/18	3.9	−89	
127	Nov. 11, 1984	T15N/R3W/18	4.7	−65	−9.7
127	Dec. 8, 1984	T15N/R3W/18	13.7	−70	−10.2
127	Jan. 19, 1985	T15N/R3W/18	3.6	−83	−11.4
127	March 30, 1985	T15N/R3W/18	9.2	−54	−9.0
150	Nov. 11, 1985	T16N/R2W/35	7.8	−62	−10.6
150	Dec. 8, 1984	T16N/R2W/35		−65	−9.4
170	Nov. 11, 1984	T15N/R1W/13	3.9	−55	
170	Jan. 19, 1985	T15N/R1W/13	2.9	−67	−9.5
170	March 30, 1985	T15N/R1W/13	7	−62	−9.3
188	Nov. 11, 1984	T15N/R4E/18	13.1	−69	−10.6
188	Jan. 19, 1985	T15N/R4E/18	4.3	−75	−10.2
188	March 30, 1985	T15N/R4E/18	9.1	−55	−9.3
200	Nov. 11, 1984	T16N/R5E/16	5.2	−72	−11.3
200	Dec. 8, 1984	T16N/R5E/16	10.6	−70	−9.3
200	Jan. 19, 1985	T16N/R5E/16	3.2	−69	−12.6
200	March 30, 1985	T16N/R5E/16	13.5P	−58	−10.1
210	Nov. 11, 1984	T16N/R6E/33	P	−77	
210	Dec. 8, 1984	T16N/R6E/33	14.0	−79	−10.2
210	Jan. 19, 1985	T16N/R6E/33	6.4	−81	−11.9
210	March 30, 1985	T16N/R6E/33	6.9P	−73	−11.0
221	Nov. 11, 1984	T16N/R7E/19	7.1	−79	−11.2
221	Dec. 8, 1984	T16N/R7E/19	12.8	−76	−12.0
221	March 30, 1985	T16N/R7E/19	18.3	−72	−12.3
221*	March 31, 1985	T16N/R7E/19	49.3P	−76	
225	Dec. 8, 1984	T16N/R8E/20	19.1	−76	−11.3
225	Jan. 19, 1985	T16N/R8E/20	6.7	−95	−13.3
225	March 30, 1985	T16N/R8E/20	30.9	−79	−11.8
232	Nov. 11, 1984	T17N/R8E/25	16.2	−75	−11.2
232	Dec. 8, 1984	T17N/R8E/25	14.4	−77	−7.1
232	Jan. 18, 1985	T17N/R8E/25	4.8	−101	−14.3
232	March 30, 1985	T17N/R8E/25	24.8	−80	−12.8
232*	March 30, 1985	T17N/R8E/25	60.5	−76	−12.5

TABLE 2. (continued)

Distance From Coast, km	Date Collected	Location	Amount of Rain Collected or Snow Depth, cm	δD_{SMOW}	$\delta^{18}O_{SMOW}$
		Traverse II, Snow			
254	April 6, 1985	T17N/R11E/30	30.5	−73	−9.6
268	April 6, 1985	T17N/R12E/30	122	−86	−12.1
272	April 6, 1985	T20N/R12E/15	30.2	−97	−13.2
280	April 6, 1985	T20N/R13E/11	152	−111	−15.2
294	April 6, 1985	T17N/R15E/8	198	−108	−15.0
295	April 6, 1985	T19N/R15E/14	76	−111	−14.7

P indicates that only a partial sample could be collected.
*Year's sample.

evapotranspiration, the system is said to be "open." In this case all water leaves the system, and downwind precipitation and therefore shallow groundwater would then become progressively depleted in D and ^{18}O. A completely "closed" system results when all of the precipitation is returned to the atmosphere by evapotranspiration, and no geographic variation in the isotopic composition of groundwater occurs. In nature, neither end-member model is entirely obtained. Deviation from the variation in δD with distance predicted by simple Rayleigh fractionation is therefore an indication of a "partially closed" system, in which some evapotranspired water is returned to the atmosphere and recycled. The "degree of closure" of the system is governed by the partitioning of precipitated water between runoff and evapotranspiration. Runoff removes water from the cloud-ground water system, while evapotranspiration retains water in the system by returning it to the atmosphere.

Figures 7*a*–7*c* schematically illustrate the geographic variation in δD of the three special systems as a function of F_v, the fraction of water vapor remaining in the atmosphere from the Rayleigh equation. An assumption that F_v varies in a regular fashion with distance inland would require a regular distribution of precipitation along the traverse. The largest isotopic variations occur in an open system dominated by Rayleigh distillation ("rain out") Figure 7*a*. In a theoretical, closed system no geographic variation in the isotopic composition of meteoric water is observed (Figure 7*b*) because all precipitation is returned to the atmosphere, and remixed. The isotopic variations of the shallow groundwater along a storm track in a partially closed system (Figure 7*c*, which may display some curvature) reflect a depletion in deuterium according to the relative magnitudes of precipitation loss as runoff and that returned via evapotranspiration. The important point here is that, at least qualitatively, steeper slopes (δD distance trends) are developed in regions where precipitation dominates evapotranspiration.

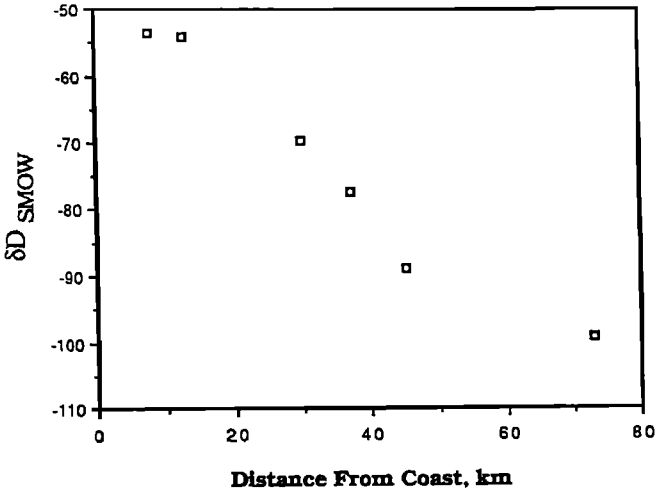

Fig. 4. Plot of δD of rain collected between January 20 and March 30, 1985, along the first 75 km of traverse I is shown with respect to distance from the Pacific Ocean.

Hydrologic Systems in California and Nevada

All of the isotopic variations characteristic of open and closed hydrologic systems (Figures 7*a*–7*c*) are observed in the hydrogen isotope data of surface waters and shallow ground waters along the traverses. Consequently, the hydrologic regimes are discussed primarily as examples of open, closed, and partially closed systems.

Open systems. The hydrologic regime of segment I-a seems to most closely approximate an open system [*Ingraham and Taylor*, 1986]. The apparent variation of δD of groundwater in segment I-a (Figure 3) suggests a dominance of rain over evapotranspiration (Figure 7*a*). The δD of precipitation (Figure 4) also indicates a dominance of rain-out in this hydrologic system and suggests a curvilinear isotopic depletion trend similar to that observed for surface waters and shallow groundwaters. The dominance of precipitation in this first regime based on isotopic data is supported by the relative proportions of measured precipitation and evapotranspiration. The coastal segments of traverses II and III, although characterized by δD distance variations with shallower slopes, also suggest that rain-out is relatively important. However, precipitation and evapotranspiration have relatively different magnitudes than measured in segment I-a. Although rain-out dominates these segments, they are considered "partially closed."

Partially closed systems. All of the coastal segments in the traverses across California are characterized by relatively steep, linear trends for δD of surface water and groundwater versus distance, and although we have suggested [*Ingraham and Taylor*, 1986] that a curved trend characterizes segment I-a, some curvature might also be suggested for II-a (Figure 3). In any case, the generally steep linearity rather than strong curvature of the first segment trends suggest partially closed systems where precipitation

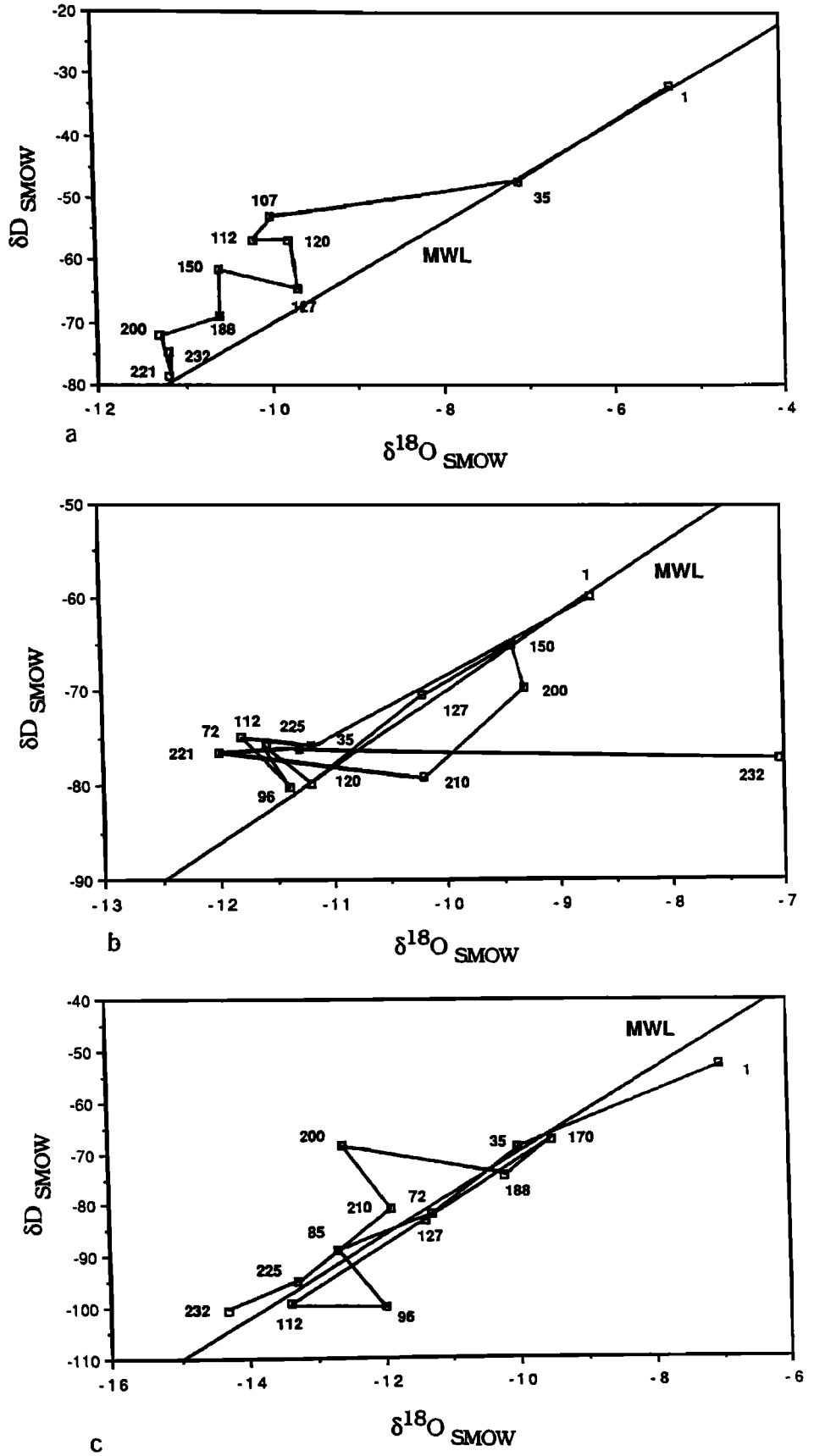

Fig. 5. Plot of the stable isotopic composition of precipitation collected along traverse II: (*a*) November 11, 1984, (*b*) December 8, 1984, (*c*) January 18, 1985, and (*d*) March 30, 1985. The numbers refer to the latitudinal distance from the Pacific Ocean in kilometers. The data points are connected in a fashion chronologically mimicking a storm as it passes across the coast and inland across the state. The meteoric water line is also shown.

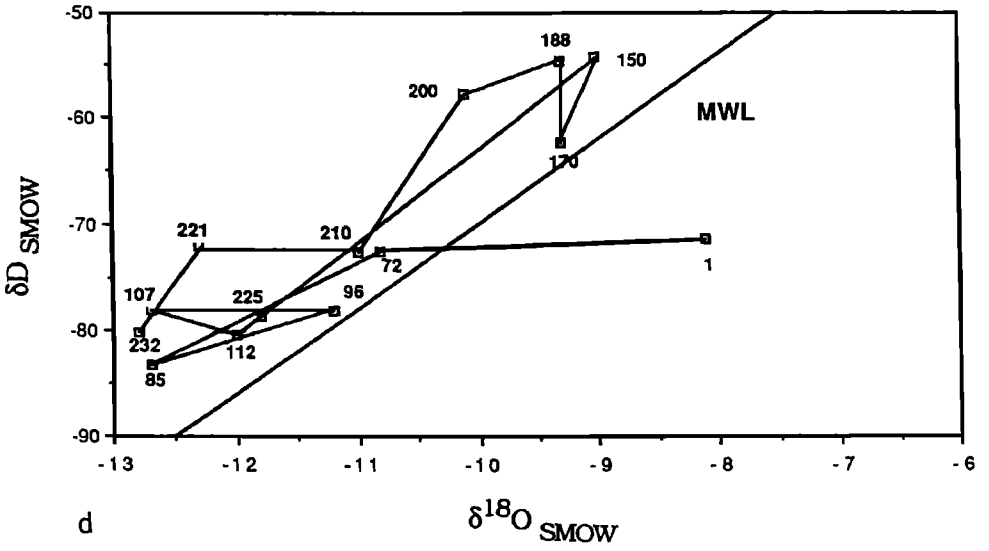

Fig. 5. (continued)

is partitioned between runoff and evapotranspiration (Figure 7c). Changes in the hydrologic regime by variations in the relative proportions of precipitation and evapotranspiration can produce different slopes for δD distance trends, as is readily apparent from traverse II (Figure 3). Approximately 100 km inland, a marked decrease in slope in the δD distance trend suggests a decrease in precipitation relative to evapotranspiration. From 0 to about 100 km, the amounts of precipitation and evapotranspiration are subequal, whereas from 100 to about 225 km, evapotranspiration dominates over precipitation. The amount of precipitation is inferred to increase relative to evapotranspiration near 225 km inland from the change in slope of the deuterium variation trend. This inference is supported by the precipitation and evapotranspiration data plotted in Figure 3 traverse II. The general validity of the isotopically based model describing the relative precipitation/evapotranspiration characteristics of the hydrologic regime thus appears to be borne out.

From approximately 100 to 280 km along traverse III (Figure 3), evapotranspiration remains fairly constant and

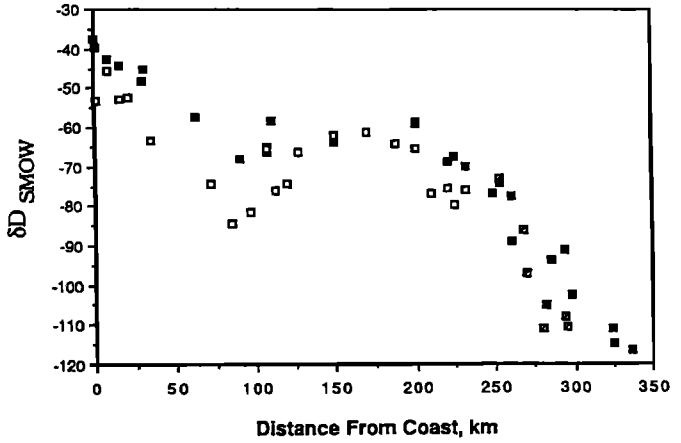

Fig. 6. Plot of the weighted average of δD of rain (open squares), snow (divided squares), and surface water and shallow groundwater (solid squares) versus distance from the Pacific Ocean collected along traverse II.

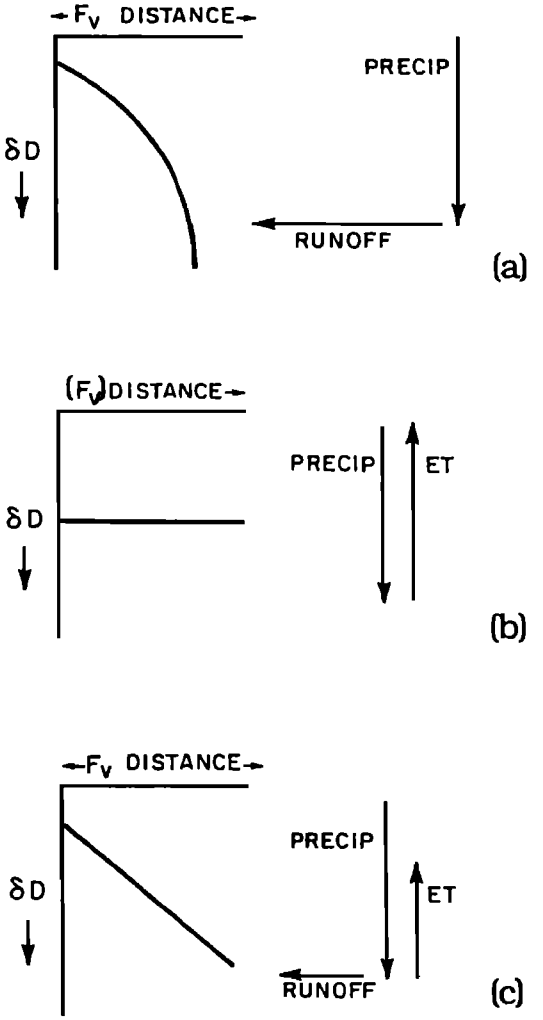

Fig. 7. Schematic of δD depletion trends for atmospheric moisture by rain-out for (a) a completely open system, (b) a closed system, and (c) a partially closed system. F_v is fraction of water vapor remaining in the "cloud system." In this model, F_v decreases as distance and cumulative precipitation increases. In a closed system, F_v is constant because there is no net water loss from the atmosphere.

greater than precipitation. Accordingly, the slope of the δD distance trend is relatively low. An increase in the precipitation/evapotranspiration ratio about 280 km inland apparently causes an increase in the slope of the δD distance trend, even though measured precipitation and evapotranspiration are indicated to be of subequal amounts.

Although the most important factor controlling the slope of deuterium depletion in a partially closed system is the ratio of precipitation to evapotranspiration, other factors must also contribute. These may include (1) temperature of precipitation, (2) the amount of water previously removed upwind, (3) modes of transpiration (e.g., type of transpiring vegetation), (4) modes of evaporation (e.g., from either soil or a free water surface), and (5) kinetic isotopic fractionation during evaporation.

Closed systems. The final three segments of each traverse, namely I-c, II-d, and III-d (Figure 3), represent the hydrologic regime of the Great Basin. At the western boundary of the Great Basin a marked change in the slope of δD versus distance is apparent along all traverses, although it is most pronounced in traverses II and III. Traverse I shows a more transitional change in slope. The δD values of groundwaters in the Great Basin are very similar within each traverse segment, with virtually no distance-dependent variation (Figure 7*b*). Most of the waters analyzed in the segments I-c, II-d, and III-d are hot springs with long recharge times and water sources at some distance (and different elevations) from the springs. As previously noted, the similarity in δD of these older waters with present-day surface waters warrants their incorporation in the model discussed here.

The low slope of δD versus distance across much of the Great Basin is compatible with the hydrologically closed nature of the Great Basin. The low δD value is accounted for by the previous loss of most of the initial moisture by precipitation. Only slight amounts of precipitation at this stage in a regional Rayleigh distillation model for an eastward moving air mass would produce relatively large variations in δD, especially if accompanied by low condensation temperatures. The isotopic data for segments I-c, II-d, and III-d suggest that this area tends to approximate both a regionally and isotopically closed hydrologic system in northern and central Nevada. The groundwater in the Great Basin is, for the most part, in isotopic equilibrium with the hydrologic systems upwind, as defined in Figure 7.

Comparison of the δD values within the most inland segments of traverses I, II, and III indicate that groundwaters in the northern and central Great Basin have δD values between −130 and −125, whereas groundwater in the southern Great Basin (segment III-d) has an average δD value of −110 (Figure 3). Thus a slight north-south isotopic gradient is apparent in the Great Basin. This gradient is primarily the result of the admixture of additional sources of atmospheric moisture with different rain-out/evapotranspiration histories.

Precipitation occurs in the southern Great Basin during both summer and winter storms [*Markham*, 1970]. The winter storms are a continuation of the eastward moving fronts from the North Pacific Ocean. Winter storm path trajectories across the Sierra Nevada produce isotopic depletion of the air mass by rain-out accentuated by elevation and the related low temperatures of winter precipitation. The summer storms pass over the warm Gulf of California [*Hales*, 1972, 1974] and more northward across southern Nevada. Figure 8 illustrates the geographic areas in which winter and/or summer precipitation dominates. In California, most of the precipitation occurs in winter, whereas in the Southwest, precipitation occurs during both winter and summer [after *Markham*, 1970]. A marked gradient in precipitation near the California-Nevada border is emphasized by the isopleth [*Horn and Bryson*, 1960] indicating a 2 : 1 ratio of winter to summer precipitation. This dual source of atmospheric moisture may be a contributory factor in controlling the relatively higher δD of surface waters and shallow groundwaters in the southern Great Basin. The isotopic effect and therefore contribution of summer-dominated precipitation in the central and northern Great Basin (segments I-c and II-d) appears to be small by comparison.

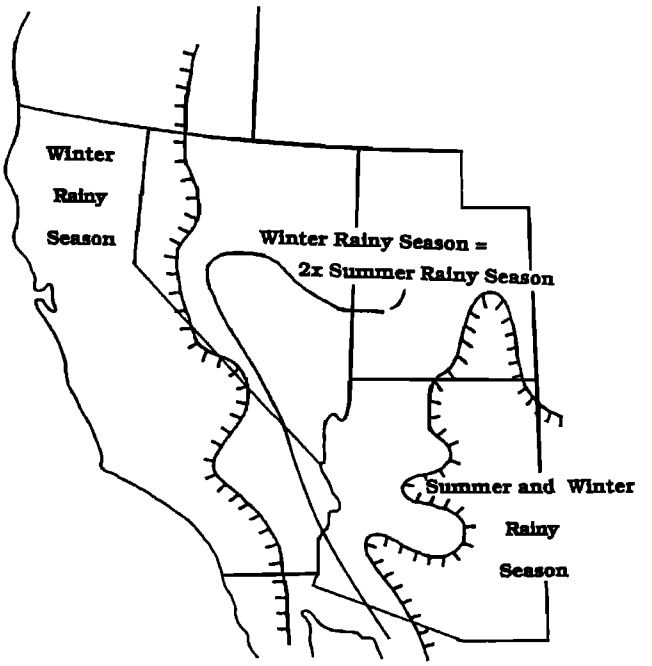

Fig. 8. The geographic dominance of the seasonal concentration of precipitation during 1951–1960. Precipitation is dominant in winter on the west coast and during winter and summer in the Southwest [after *Markham*, 1970]. Also shown is the location where the ratio of the amount of winter to summer precipitation is 2 : 1 [after *Horn and Bryson*, 1960].

Application to California's Water Balance

The amount of terrestrial water recycled in a region can be estimated from a simple precipitation/evapotranspiration model. This model incorporated measured hydrogen isotope data on the coast, predicts the hydrogen isotope compositions above the crest of the Sierra Nevada after pseudoadiabatic cooling of eastward moving moisture, and demonstrates that recycled meteoric water is an important source for inland waters. Further, the model develops a baseline for comparison by calculating the total isotopic change accompanying precipitation in a completely open system. Several simplifying assumptions in the model are (1) water contributed to the atmospheric vapor over the North Pacific Ocean was originally in isotopic equilibrium with the ocean at 10°C, (2) the atmosphere is vertically well mixed, (3) precipitation occurs under equilibrium conditions, (4) precipitation con-

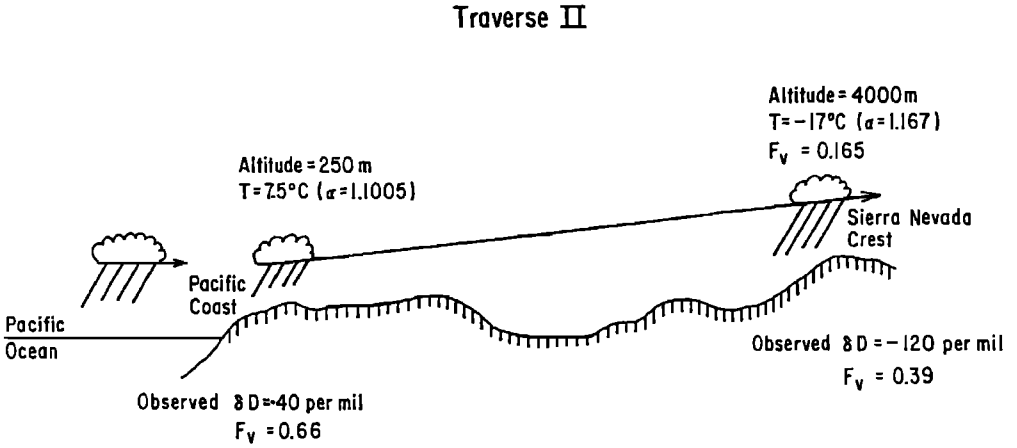

Fig. 9. Diagram of the "lifting cloud" model is diagrammed for traverse II. Observed hydrogen isotopic compositions of groundwater at the coast is −40‰. Assuming a first precipitate over the ocean of 0‰, and a condensation temperature of 7.5°C (alpha = 1.1005), an F_v for the cloud of 0.6 is determined. This cloud is then lifted to 1500 m above the Sierra crest (to 4000 m) where it condenses out snow at −17°C (alpha = 1.167) with an F_v of 0.17. The cloud would now produce a precipitate of −217‰. However, groundwater at the crest is observed to have a δD of only −120‰, which corresponds (at −17°C) to an F_v of 0.39. The discrepancy between the two F_v values (0.17 and 0.39) is 0.22, which is interpreted to be the fraction of recycled water required to produce the observed hydrogen isotopic compositions of groundwater at the crest.

sists of rain at formation temperatures above 0°C, rain and snow between 0°C and −15°C, and snow below −15°C, and (5) the isotopic compositions of rain and snow represent conditions at 250 and 1500 m, respectively, above the ground surface.

This model and results of calculations for traverse II are shown in Figure 9. Because water evaporated from the ocean yields a precipitate with a δD value of close to 0, significant precipitation from the storm track prior to reaching land is required to explain the δD values of −40 at the beginning of traverse II. The fraction of initial water vapor remaining in the cloud system (F_v) is 0.66 from the Rayleigh equation. As the eastward moving storm clouds rise pseudoadiabatically to the crest of the Sierra Nevada, they lose water along the way, further depleting the atmosphere in deuterium. In a simple rain-out process the predicted isotopic composition of precipitation (snow) at the crest is δD = −217, as shown for traverse II in Figure 9. Similarly, this "lifting cloud" calculation was also applied to traverses I and III, and the results are listed in Table 3.

Storm systems crossing the coast contain between 60% (F_v = 0.60, traverse I) and 70% (F_v = 0.70, traverse III) of the original water vapor, based on the δD of coastal groundwaters. Mixing ratios (in grams of water per kilogram of dry air) and saturated temperatures were calculated for F_v = 1.0 (inception of storm) to evaluate whether the assumption of 30–40% water loss over the ocean is reasonable. The resulting saturation temperatures were between 12.5°C and 15°C (Table 3). The predicted δD and F_v values for snow at the Sierra Nevada crest by this "lifting cloud" model are given with the measured δD value of ground water at the crest in Table 3. Values of F_v calculated from the Rayleigh equation constrained by the measured δD values are lower by comparison; a result of water recycling as described below.

The discrepancies in F_v and between predicted and measured δD values for each traverse listed in Table 3 imply

TABLE 3. Calculation of F_v at the Sierra Nevada Crest

Method	Parameters	Traverse I	Traverse II	Traverse III
1	observed δD of groundwater at the coast (‰)	−50	−40	−33
	calculated F_v at the coast	0.60	0.66	0.70
	mixing ratio at F_v = 1.0 (inception of storm)	10.8	9.75	9.0
	saturation temperature at F_v = 1.0	15°C	13°C	12.5°C
	elevation at the Sierra Nevada crest, m	2100	2500	4400
	altitude of precipitation formation at the crest, m	3600	4000	5900
	temperature of precipitation formation at the crest	−14°C	−17°C	−32°C
	fractionation factor α at the crest	1.158	1.167	1.204
	predicted δD of precipitation at the crest, ‰	−194	−217	−379
	F_v at the crest by pseudoadiabatic calculations	0.19	0.17	0.06
2	observed δD of meteoric water at the crest, ‰	−120	−120	−125
	F_v needed to produce the observed δD at the crest	0.37	0.39	0.45
	Discrepancy in F_v between observed and calculated δD (amount of water recycled)	0.18	0.22	0.39

F_v, fraction of water vapor remaining in the cloud system; 1, water loss calculated by psuedoadiabatic means; 2, water loss calculated by measurements of the hydrogen isotopic compositions of groundwater at the crest.

upwind recycling by evapotranspiration. Differences in F_v vary between 0.18 and 0.39, and the differences in δD predicted for precipitation at the crest of the Sierra Nevada range from 74 to 254‰. Although minor changes in the differences would result from adjusting the initial assumptions of temperature, elevation of isotopic equilibrium, etc, it is evident that isotopic variations associated with rain-out are moderated by recycling. The recycling process would also probably include the evaporation of rain during descent and partial evaporation of meltwater prior to infiltration.

CONCLUSIONS

Groundwater, surface water, and precipitation were collected along three traverses, aligned parallel to the atmospheric flow path, across northern California and Nevada. The hydrogen isotope compositions of individual precipitation events were found to be highly variable and not representative of the average hydrogen isotope composition of precipitation. However, the weighted yearly average of precipitation more accurately reflects the nature of the hydrologic regime, as represented by the δD values of shallow groundwater.

The traverses were divided into distinct segments based on the variations in δD of surface water and shallow groundwater. Variations of δD within chosen segments indicate hydrologic regimes that correlate with relative differences in the vertical fluxes of meteoric water estimated from measured evapotranspiration and precipitation data. The roughly linear trends of δD versus distance of most segments approximate partially closed systems in which precipitation is partitioned between runoff and evapotranspiration. Different slopes of these trends, for the most part, represent different relative contributions of evapotranspiration and precipitation. One coastal segment appears to closely represent an open system where precipitation is greater than evapotranspiration, and water is removed via runoff.

Partially closed systems require terrestrial recycling of meteoric water by evaporation and transpiration to explain the geographic variation in δD of inland meteoric water. A simple model suggests about 20% terrestrial moisture is recycled via evapotranspiration across northern and central California.

The isotopic composition of meteoric water is shown to be directly related to the closure of the hydrologic system(s) upwind. A small change in the "degree of closure" of the hydrologic system (i.e., a change in the relative amounts of precipitation and runoff or evapotranspiration) upwind may produce substantial changes in the isotopic composition of inland meteoric water.

Acknowledgments. This research was supported by the State Water Resources Research Institute, project 569986-28558-3, and by the University of California Water Resources Center, project UCAL-WRC-W-656. Additional funding was provided by a Grant-in-Aid of Research from Sigma Xi. J. R. O'Neil (U.S.G.S., Menlo Park, California) kindly permitted use of the mass spectrometer for hydrogen isotope analyses, and J. Hess (Desert Research Institute, Las Vegas, Nevada) allowed use of the DRI isotope laboratory for some of the oxygen isotope analyses. T. Coplen (U.S.G.S., Reston, Virginia) kindly supplied several duplicate oxygen and hydrogen isotope analyses.

REFERENCES

Bigeleisen, J., M. L. Perlman, and H. Prosser, Conversion of hydrogenic materials to hydrogen for isotopic analysis, *Anal. Chem.*, *24*, 1356–1357, 1952.

Craig, H., Isotope variations in meteoric waters, *Science*, *133*, 1702–1703, 1961.

Dansgaard, W., Stable isotopes in precipitation, *Tellus*, *16*, 436–438, 1964.

Dugan, J. P., Jr., J. Borthwick, R. S. Harmon, M. A. Gagnier, J. E. Gahn, E. P. Kinsel, S. Macleod, J. A. Viglino, and J. W. Hess, Guanidine hydrochloride method for determination of water oxygen isotope ratios and the oxygen-18 fractionation between carbon dioxide and water at 25°C, *Anal. Chem.*, *57*, 1734–1736, 1985.

Epstein, S., and T. K. Mayeda, Variations on ^{18}O contents of waters from natural sources, *Geochim Cosmochim Acta*, *4*, 213–214, 1953.

Friedman, I., and J. O'Neil, Data of geochemistry, compilation of stable isotopic fractionation factors of geochemical interest, *U.S. Geol. Surv. Prof. Pap.*, *440KK*, 1977.

Friedman, I., and G. I. Smith, Deuterium content of snow cores from Sierra Nevada area, *Science*, *169*, 467–470, 1970.

Friedman, I., and G. I. Smith, Deuterium content of snow as an index to winter climate in the Sierra Nevada area, *Science*, *176*, 790–793, 1972.

Friedman, I., A. C. Redfield, B. Shoem, and J. Harris, The variations of the deuterium content of natural waters in the hydrologic cycle, *Rev. Geophys.*, *2*, 177–224, 1964.

Goodridge, J. D., K. Jones, W. Mancibo, C. K. Muir, D. Schuder, E. W. Danley, P. Schreiner, E. G. Bingham, and S. Midson, California rainfall study, monthly total precipitation 1849–1980, 41 pp., Calif. Dep. of Water Resour., Sacramento, 1981.

Hales, J. E., Jr., Surges of maritime tropical air northward over the gulf of California, *Mon. Weather Rev.*, *100*(4), 298–306, 1972.

Hales, J. E., Jr., Southern United States summer monsoon source–Gulf of Mexico or Pacific Ocean, *J. Appl. Meteorol.*, *13*, 331–342, 1974.

Horn, L. H., and R. A. Bryson, Harmonic analysis of the annual march of precipitation over the United States, *Ann. Assoc. Am. Geog.*, *50*, 157–171, 1960.

Ingraham, N. L., and B. E. Taylor, Hydrogen isotope study of large-scale meteoric water transport in Northern California and Nevada, *J. Hydrol.*, *85*, 183–197, 1986.

Jacobson, R. L., N. L. Ingraham, and M. E. Campana, Isotope hydrology of a Basin and Range geothermal system, *Publ. 41807*, Desert Res. Inst., Univ. of Nev., Las Vegas, 1983.

Kendall, C., and T. Coplen, Multisample conversion of water to hydrogen by zinc for stable isotope determination, *Anal. Chem.*, *57*, 1437–1440, 1985.

MacGillivray, N. A., R. R. McGill, J. H. Lawrence, F. E. Stumpf, R. D. Smith, C. K. Muir, W. G. McKane, T. Latham, and J. D. Goodridge, Vegetative water use in California, 1974, *Bull. 113-3*, 104 pp., Calif. Dep. of Water Resour., Sacramento, 1975.

Mariner, R. H., T. S. Presser, J. B. Rapp, and L. M. Willey, The minor and trace elements, gas, and isotope compositions of the principal hot springs in Nevada and Oregon, *U.S. Geological Survey Open File Rep.*, 1975.

Mariner, R. H., T. S. Presser, and W. C. Evans, Geochemistry of active geothermal systems in northern Basin and Range province, *Spec. Rep. 13*, pp. 95–119, Geothermal Resour. Counc., Davis, Calif., 1983.

Markham, C. G., Seasonality of precipitation in the United States, *Ann. Assoc. Am. Geogr.*, *60*, 593–597, 1970.

Merlivat, L., and J. Jouzel, Global climatic interpretation of the deuterium-oxygen-18 relationship for precipitation, *J. Geophys. Res.*, *84*, 5029–5033, 1979.

Reed, M. J., Chemistry of thermal waters in selected geothermal areas of California, *Rep. TR-15*, Calif. Div. of Oil and Gas, San Francisco, 1975.

Rozanski, K., Deuterium and oxygen-18 in European groundwaters–Links to atmospheric circulation in the past, *Chem. Geol.*, *52*, 349–363, 1985.

Rozanski, K., K. O. Munnich, and C. Sonntag, Modelling of stable isotope composition of atmospheric water vapour and precipitation in *Stable Isotopes*, edited by H. L. Schmidt, H. Foerstel, and K. Heinzinger, Elsevier, New York, 1982*a*.

Rozanski, K., C. Sonntag, and K. C. Munnich, Factors controlling stable isotope composition of European precipitation, *Tellus*, *34*, 142–150, 1982*b*.

Salati, E., A. Dall'Olio, E. Matsui, and J. R. Gat, Recycling of water

in the Amazon basin: An isotopic study, *Water Resour. Res.*, *15*, 1250–1258, 1979.

Smith, G. I., I. Friedman, H. Klieforth, and K. Hardcastle, Areal distribution of deuterium in eastern California precipitation, 1968–1969, *J. App. Meteorol.*, *18*, 172–188, 1979.

Truesdell, A. H., M. Nathenson, and R. O. Rye, The effects of subsurface boiling and dilution on the isotopic composition of Yellowstone thermal waters, *J. Geophys. Res.*, *82*, 3694–3703, 1977.

Yonge, C. J., L. Goldberg, and H. R. Krouse, An isotopic study of water bodies along a traverse of Southwestern Canada, *J. Hydrol.*, *106*, 245–255, 1989.

Waddell, R. K., J. H. Robinson, and R. K. Blankennagel, Hydrology of Yucca Mountain and vicinity, Nevada-California investigative results through mid-1983, *U.S. Geological Survey Water Resources Invest. Rep.*, *84-4267*, 1984.

N. L. Ingraham, Water Resources Center, Desert Research Institute, University of Nevada, 2505 Chandler Avenue, Las Vegas, NV 89120.

B. E. Taylor, Geological Survey of Canada, 601 Booth Street, Ottawa, Ontario, K1A 0E8, Canada.

(Received March 27, 1989;
revised May 21, 1990;
accepted June 23, 1990.)